Communication

Low-Profile and Wideband Microstrip Antenna Using Quasi-Periodic Aperture and Slot-to-CPW Transition

Wangyu Sun[®], Yue Li[®], Zhijun Zhang[®], and Pai-Yen Chen

Abstract—In this communication, we propose a new type of compact and wideband coplanar waveguide (CPW)-fed microstrip antenna. Very different from traditional microstrip antennas, the proposed design has the quasi-periodic radiating aperture fed through the slot-to-CPW transition. By optimizing the geometry of the quasi-periodic aperture and the slot-to-CPW transition, the fundamental TM₁₀ mode and antiphase TM₂₀ mode can be efficiently excited, coupled, and matched over a broad bandwidth. We have fabricated and characterized the proposed antenna, and found a good agreement between measurement and simulation results. Our experimental results show that despite the antenna has a thickness of only $0.052\lambda_0$ (λ_0 is the free-space wavelength at the center frequency), it exhibits a -10 dB impedance bandwidth of 36.5% (3.96-5.73 GHz), a 3 dB gain bandwidth of 35.4% (4-5.72 GHz), and a maximum available gain of 10.45 dBi. Our findings may offer a feasible solution to realize wideband microstrip antennas using a single-layer substrate, with unique merits, such as low profile, low cost, and ease of fabrication.

Index Terms—Antenna feeds, broadband antennas, impedance matching, low-profile antennas, microstrip antennas.

I. Introduction

Microstrip antennas have attracted tremendous attention in the past several decades, due to the advantages of low cost, low profile, lightweight, and conformability to mounting devices [1]. However, their practical uses in modern wideband communications systems are limited by the intrinsically narrow bandwidth, owning to the high quality-factor (Q-factor) of compact microstrip antennas [2]. How to enhance the bandwidth of microstrip antennas, while maintaining their compact size, has recently become an emerging research hotspot. To date, several techniques have been proposed to enhance the bandwidth of microstrip antennas. One intuitive approach is to use a thick dielectric substrate with low permittivity, which helps lowering the effective Q-factor of the cavity structure [3]. In addition, various capacitive feeding schemes, such as L-shape [4] and meandering probes [5], have been proposed to enlarge the bandwidth of microstrip antennas with a profile of $\sim 0.1\lambda_0$. The E-shaped microstrip patch antennas have also been proposed to achieve a bandwidth of 9% (24%), with a profile of only $0.043\lambda_0$ [6] ($0.08\lambda_0$ [7]). The bandwidth of the E-shaped patch antenna can be further improved to 34% by integrating the planar antenna with the SIW cavity and the coplanar waveguide (CPW) feed [8]. Inspired by these works, different kinds of slot etched on the microstrip patch (e.g., H-shaped slot [9] and

Manuscript received June 4, 2018; revised September 23, 2018; accepted October 1, 2018. Date of publication October 9, 2018; date of current version January 16, 2019. This work was supported in part by the National Natural Science Foundation of China under Grant 61771280 and in part by the Natural Science Foundation of Beijing Manipulate under Contract 4182029. (Corresponding author: Yue Li.)

W. Sun, Y. Li, and Z. Zhang are with the Department of Electronic Engineering, Tsinghua University, Beijing 100084, China (e-mail: lyee@tsinghua.edu.cn).

P.-Y. Chen is with the Department of Electrical and Computer Engineering, University of Illinois at Chicago, Chicago, IL 60607 USA.

Color versions of one or more of the figures in this communication are available online at http://ieeexplore.ieee.org.

Digital Object Identifier 10.1109/TAP.2018.2874801

U-shaped [10] slot) have been studied to improve the bandwidth of the microstrip antenna. However, most of these antenna structures have asymmetric current distributions, thus exhibiting increased cross-polarized radiations. Hybridizing different resonant modes in a microstrip cavity may also increase the bandwidth of operation. As demonstrated in [11]–[14], multilayered microstrip antennas comprising stacked patches of different sizes can generate multiple resonant modes such that a bandwidth of 10.5% can be achieved [11]. In the extended studies, bandwidths of 22%, 35%, and 39% have been demonstrated by using the aperture-coupled antennas of different parasitic patch geometries [12]–[14]. Unfortunately, the price paid for the enhanced bandwidth is a significantly increased profile, typically greater than $0.13\lambda_0$.

Apart from approaches mentioned earlier, a new technique inspired by the multimodes coupling theory has recently been reported to enhance the operating bandwidth (while maintaining a low profile [15]-[25]). Such an approach relies on exciting multiple resonant modes in a single microstrip patch cavity. With a very low profile of $\sim 0.01\lambda_0$, a narrow bandwidth of 3.8% can be achieved by simultaneously exciting the orthogonal TM₁₀ and TM₀₁ modes [15]. It has been demonstrated in [16] that an alternative triangular patch operating at the TM₁₀ and TM₂₀ modes, although having a slightly larger profile $\sim 0.09\lambda_0$, shows an enhanced bandwidth of 32.2%. Besides, it has been demonstrated in [17] and [18] that by allocating TM₁₀ and TM₃₀ modes in proximity to each other via etched slots and shorting pins, bandwidths of 15.5% [17] and 13% [18] can be achieved, with a low profile $\sim 0.03 \lambda_0$. The grid-slotted radiating patches inspired by metasurfaces [19]-[23] have also been demonstrated to achieve a large bandwidth (>30%), with a profile of $\sim 0.06 \lambda_0$. In general, these techniques require complex and costly multilayer substrate. A similar idea of multiple parallel resonators has also been studied in [24] and [25], of which reconfigurable pixel patches were used to enhance the bandwidth of operation. However, loading the passive antenna with switches could increase the cost, noise, and fabrication complexity.

In this communication, we propose a wideband and low-profile gap-loaded microstrip antenna, employing the quasi-periodic aperture and the slot-to-CPW transition depicted in Fig. 1(a). The quasi-periodic aperture is constructed by four discrete strips with subwavelength air gaps. Such a radiating aperture can co-excite the fundamental TM₁₀ mode and the antiphase TM₂₀ mode (evenorder mode). Interestingly, the even-order mode that is suppressed by inherent boundary conditions in traditional microstrip antennas can be excited in our design. Here, a suitably designed slot-to-CPW transition is used to excite both resonant modes, such that the antenna can be built based on an inexpensive single-layer substrate. On the other hand, the co-excitation of these two modes in other microstrip apertures usually requires a substrate of at least two layers [19]-[23]. By optimizing the quasi-periodic aperture and the slot-to-CPW transition of the proposed antenna, the TM₁₀ and antiphase TM₂₀ modes can be coupled together to achieve a broader

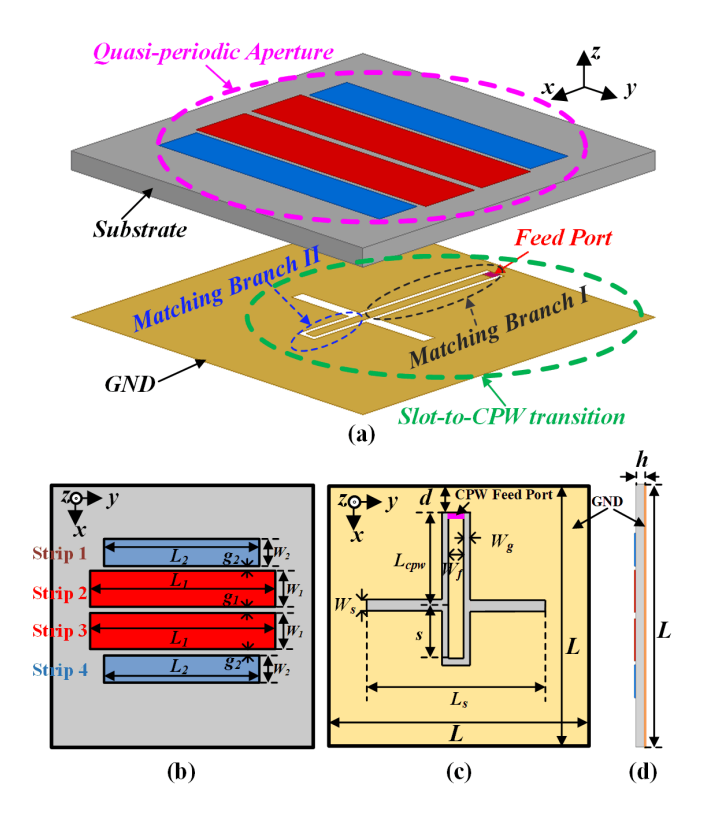


Fig. 1. Geometry and dimensions of the proposed microstrip antenna. (a) 3-D view and (b) top view with the quasi-periodic aperture. (c) Bottom view of the slot-to-CPW transition. (d) Side view of the antenna.

bandwidth and an improved impedance matching, when compared to conventional microstrip antennas. We have built and fully characterized the proposed antenna. Our experimental results show that the -10 dB impedance bandwidth is about 36.5%, with a very low antenna profile of only $0.052\lambda_0$.

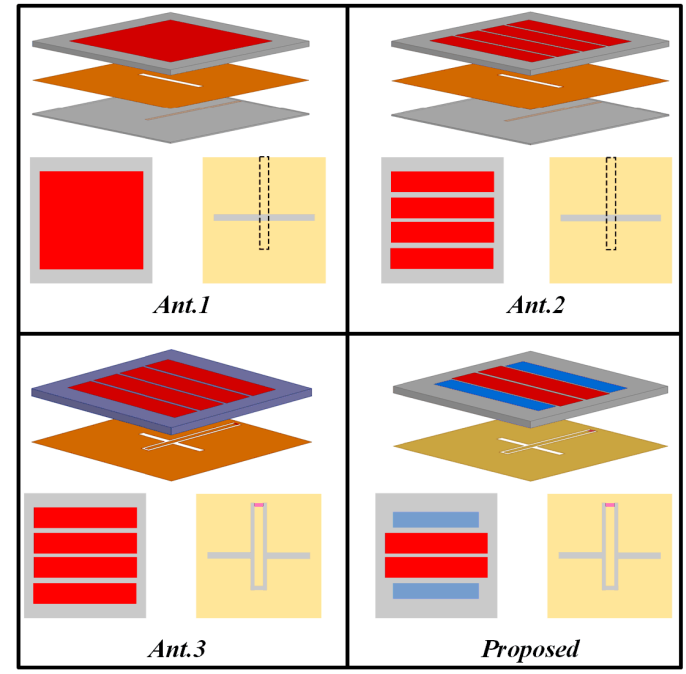
II. CONFIGURATION AND OPERATING CONCEPTS

Fig. 1(a) presents the geometry of the proposed quasi-periodic microstrip antenna on a grounded dielectric substrate, which has a relative permittivity of 3.38 and a loss tangent of 0.009. The quasiperiodic aperture consists of four rectangular strips with slightly different sizes, which are separated by air gaps, as shown in Fig. 1(b). In our design, strip 2 and strip 3 (strip 1 and strip 4) have the same dimension of $W_1 \times L_1$ ($W_2 \times L_2$). The middle (g_1) and edge (g_2) gaps also have different sizes. In the bottom layer of the substrate, a novel slot-to-CPW transition is printed to feed this gap-loaded microstrip patch (i.e., radiating aperture). The slot-to-CPW transition transmits and couples the energy from the CPW to the radiating aperture through the center slot, as shown in Fig. 1. Details of the slot-to-CPW transition are shown in Fig. 1(c), which contains four parts: center slot, matching branch I, matching branch II, and feed port. The center slot with a dimension of $W_S \times L_S$ is cut on the ground plane and seated underneath the middle gap of the radiating aperture. The two matching branches lie along the x-axis, and lengths of matching branch I and matching branch II are L_{cpw} and s. The width of center feed line is W_f . The width of the gap between the center feed line and ground is W_g . The coaxial cable with a characteristic impedance of 50 Ω is used to feed such a single-layered microstrip antenna. The distance between the feed port and the edge of the ground plane is d $(d = L/2 - L_{cpw})$. All design parameters used here are summarized

TABLE I

DIMENSIONS OF THE ANTENNA IN FIG. 1 (UNIT: MM)

L =68	$L_1 = 52$	L ₂ =50	$W_1 = 11$	W ₂ =8.5	$g_1 = 1.6$	$g_2=1$
$W_s = 2.5$	$L_s = 30$	s=12	$L_{cpw}=32$	$W_g = 0.6$	$W_f=2$	h =3.25



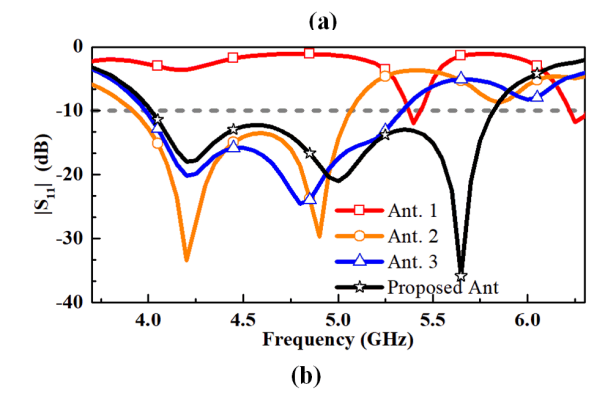


Fig. 2. (a) Design steps of the proposed antenna. (b) Evolution trend of $|S_{11}|$ with different antennas.

in Table I, whose values are obtained by the numerical optimization using high-frequency structure simulator.

A. Evolution Processes

To illustrate the design concept, we have studied four different types of antennas with similar structures. Their structural evolution is shown in Fig. 2(a). In general, microstrip antennas are fed by a microstrip line through the coupling slot etched on the ground plane. However, this method, represented as "microstrip feed" (MSF), requires a substrate of at least two dielectric layers and three metal layers [17], [20]. Ant. 1 in Fig. 2(a) is the traditional slot-coupled microstrip antenna, comprising a square patch and an MSF. Ant. 2 is modified from Ant. 1, but with a periodic aperture composed

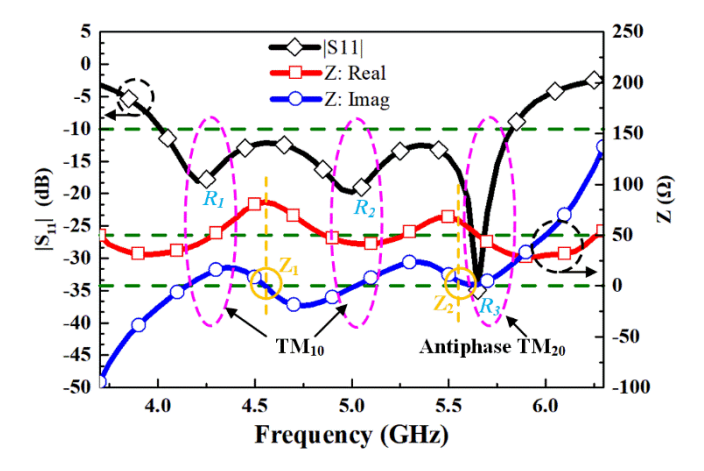


Fig. 3. Simulated $|S_{11}|$ and complex impedance of the proposed antenna [Ant. 4 in Fig. 2(a)].

of identical strips and gaps. Ant. 3 is modified from Ant. 2, but with the proposed slot-to-CPW feeding structure. Finally, Ant. 4 is the proposed quasi-periodic microstrip antenna, with its aperture made of nonuniform gaps and strips. The reflection coefficients of the four antennas are shown in Fig. 2(b).

For a conventional square patch (i.e., Ant. 1), the magnitude of the electric field is 0 at the center and reaches its maximum at the two edges. Therefore, only odd modes can be excited and even modes are largely suppressed, due to the enforced boundary condition in the cavity model. Besides, the resonant frequencies of two adjacent odd modes are usually far apart from each other. Hence, Ant. 1 has a narrow -10 dB bandwidth, as shown in Fig. 2(b). To enhance the impedance bandwidth through the multimode coupling, Ant. 2 consists of a square patch loaded with three uniform air gaps. The center gap on this periodic aperture provides the feasible boundary condition to support the antiphase TM₂₀ mode. Besides, the gaps between adjacent strips behave as the capacitive loading, which also contribute to the bandwidth enhancement. From Fig. 2(b), we observe that Ant. 2 exhibits a dual-resonant behavior with two resonant frequencies 4.2 and 4.8 GHz, which correspond to the TM₁₀ and antiphase TM₂₀ mode. By coupling these two neighboring resonant modes, Ant. 2 can achieve a wider -10 dB impedance bandwidth of 3.91–5.06 GHz, (25.6%), compared to the traditional one (i.e., Ant. 1). Since Ant. 2 is based on the MSF structure, it still requires a two-layer substrate. To further improve the radiation performance and bandwidth, Ant. 3 adopts the proposed slot-to-CPW transition. Due to the coplanar configuration of CPW [26], [27], Ant. 3 is based on the single-layer substrate. Besides, this feeding structure introduces two matching branches and three additional tuning parameters, which may further broaden the impedance bandwidth. By optimizing geometries of the slot-to-CPW transition, Ant. 3 can have a broader impedance bandwidth than Ant. 2. Our simulation results show that the bandwidth of Ant. 3 can be improved to 3.98-5.34 GHz (29.2%), as shown in the blue line in Fig. 2(b). The introduction of the quasi-periodic aperture (Ant. 4) offers additional design flexibility for impedance matching. As shown in the black line in Fig. 2(b), Ant. 4 exhibits three resonant modes at 4.2, 5, and 5.65 GHz, and the largest bandwidth of 4.01-5.82 GHz (36.8%) among different types of microstrip antennas in Fig. 2(a).

B. Operating Mechanism

Fig. 3 shows the simulated $|S_{11}|$ and the complex input impedance $(R_{in} + jX_{in})$ for the proposed antenna (Ant. 4). The three resonant

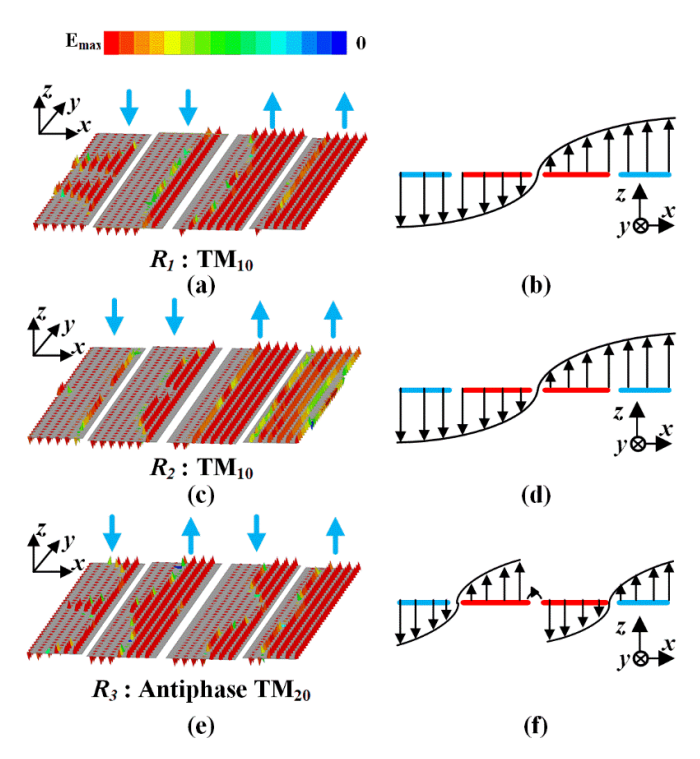


Fig. 4. Vector electric field distributions on the xy plane. Sketches of field distributions along the x-axis at (a) and (b) R_1 , (c) and (d) R_2 , and (e) and (f) R_3 ; here, R_1 , R_2 , and R_3 are resonant frequencies denoted in Fig. 3.

frequencies are marked as R_1 , R_2 , and R_3 , corresponding to 4.2, 5, and 5.65 GHz. At resonant frequencies of a microstrip antenna, one may obtain $X_{\rm in}=0$ and a negative-slope dispersion [17]. From Fig. 3, we find that there are only two resonant modes Z_1 and Z_2 , which achieve $X_{\rm in}=0$ and negative slopes. The frequency of the resonant mode Z_2 is close to the resonant frequency R_3 , whereas the frequency of the resonant mode Z_1 is located between R_1 and R_2 . This depicts that the resonant frequency R_3 solely works at the resonant mode Z_2 , but resonant frequencies R_1 and R_2 both work at the resonant mode Z_1 .

The operating modes at three resonant frequencies are depicted using the vector electric field distributions on the xy plane, as shown in Fig. 4(a), (c), and (e). We find that almost identical distributions are excited at R_1 and R_2 (i.e., the same resonant mode Z_1), agreeing well with the phenomenon observed from the dispersion of X_{in} in Fig. 3. The vector electric field exhibits the "half-wavelength" resonance along the x-axis and the uniform distribution along the y-axis. The schematics along the x-axis are given in Fig. 4(b) and (d), analogous to TM₁₀ mode in the classical microstrip patch antenna. At the resonant frequency R_3 , the vector electric field displays the "onewavelength" resonance along the x-axis and uniform distributions along the y-axis, as shown in Fig. 4(e). The schematic along the x-axis is shown in Fig. 4(f). The electric fields are out-of-phase in the middle gap with the antiphase TM20 mode excited at the resonant frequency R_3 . This is very different from TM_{20} mode in the classical microstrip patch antenna. It is worth mentioning that the resonant modes at R_1 and R_2 intrinsically exist in the quasi-periodic cavity structure, whereas the resonant mode at R_3 is contributed by interactions between the radiating aperture and the CPW-to-slot transition. By optimizing the sizes of the quasi-periodic aperture and the slot-to-CPW transition, these three resonant frequencies operating

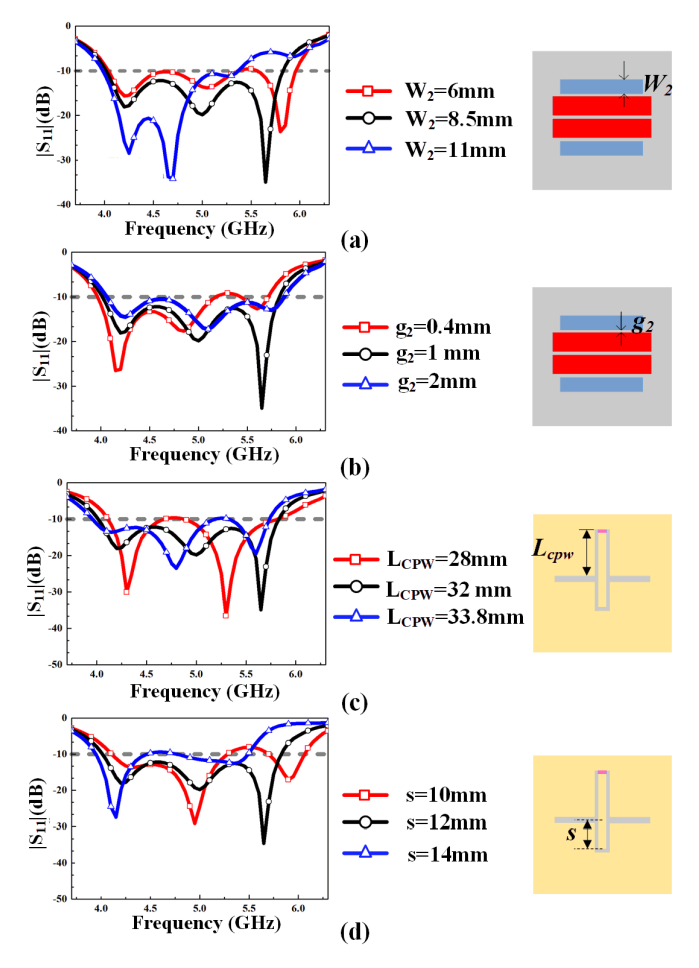


Fig. 5. Simulated $|S_{11}|$ for the proposed antenna with different values of (a) W_2 , (b) g_2 , (c) L_{cpw} , and (d) s.

at TM_{10} and antiphase TM_{20} modes can be co-excited, coupled, and well matched for achieving a wide bandwidth of 36.8%.

III. PARAMETER STUDIES

For the proposed microstrip antenna (Ant 4), each strip forming the quasi-periodic aperture can be seen as an inductive element, and the inductance of strip 1 and strip 4 can be tuned by varying the strip width W_2 . Besides, each gap in the quasi-periodic aperture can be seen as a capacitive element, with its effective capacitance being varied by the gap size g_2 . Thus, by properly adjusting W_2 and g2, the effective inductance and capacitance of the radiating aperture can be tuned to achieve the optimum impedance matching condition. Fig. 5(a) and (b) shows the $|S_{11}|$ spectrum for the proposed antenna, with W_2 and g_2 being swept. From the numerical results, we find that optimal design parameters are $W_2 = 8.5 \text{ mm}$ and $g_2 = 1 \text{ mm}$, which give satisfactory impedance matching and bandwidth. For the slot-to-CPW transition, matching branch I can be regarded as an impedance transformer. By adjusting the length of the matching branch I (L_{cnin}) , the impedance matching between the exciting port and the coupling slot can be improved, and so does the bandwidth of the antenna. Matching branch II is an open stub behaving as a capacitive load. By adjusting the length of matching branch II (s), the value of loaded capacitance can be tuned to achieve the optimum impedance matching condition. Fig. 5(c) and (d) presents the trends of the $|S_{11}|$ spectrum for the proposed antenna, with L_{cpw} and s being swept. As observed from numerical results, we choose $L_{cpw} = 32$ mm and s = 12 mm, which give the optimum matching condition. With the optimal set of

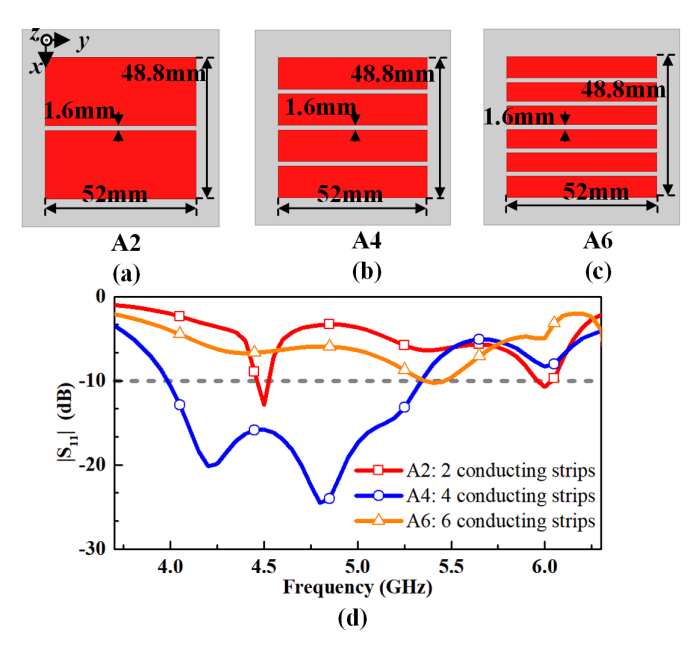


Fig. 6. (a)–(c) Geometries and (d) simulated $|S_{11}|$ curves of three quasi-periodic microstrip antennas with different numbers of rectangular strips.

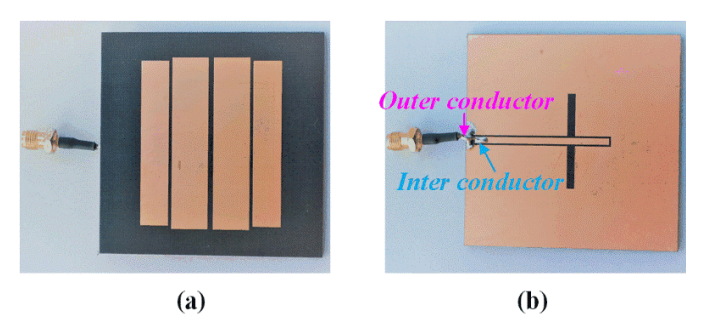


Fig. 7. Photograph of the proposed antenna. (a) Top view. (b) Bottom view.

 (W_2, g_2, L_{cpw}, s) , three resonant frequencies $(R_1, R_2, \text{ and } R_3)$ can be excited and well matched, resulting in a wide impedance bandwidth.

We have also studied the effect of the number of rectangular strip. Fig. 6(a)–(c) presents the periodic microstrip antennas with 2, 4, and 6 rectangular strips; here, except for the number of strip, all design parameters are fixed. Fig. 6(d) presents the simulated results for such antennas, showing that the periodic microstrip antenna with four discrete strips has the widest bandwidth.

In the following, we provide a detailed guideline to implement the proposed quasi-periodic microstrip antenna.

Step 1: Construct a conventional slot-coupled microstrip-fed antenna, of which the size of the square patch is estimated according to the center frequency f_0 and the substrate permittivity.

Step 2: Notch three gaps on the square patch to construct the periodic aperture and optimize the size to excite TM_{10} mode and the antiphase TM_{20} mode.

Step 3: Transform the microstrip feed to the slot-to-CPW transition and adjust the two matching branches for impedance matching.

Step 4: Transform the periodic aperture to the quasi-periodic aperture by perturbing the size of each strip and gap, in order to further enhance the impedance bandwidth.

IV. FABRICATION AND MEASUREMENT

Here, we also fabricated and measured the proposed quasiperiodic microstrip antenna, with dimensions listed in Table I.

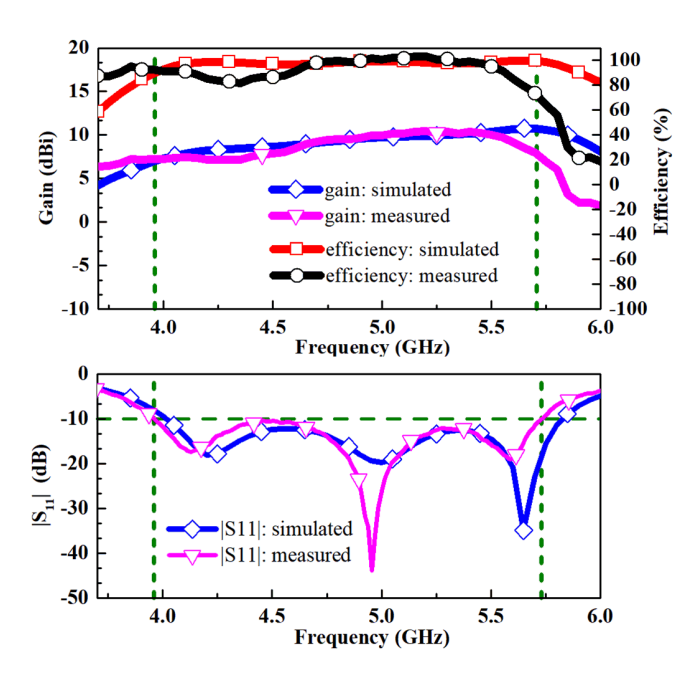


Fig. 8. Simulated and measured gain, radiation efficiency, and $|S_{11}|$ curves of the proposed quasi-periodic microstrip antenna.

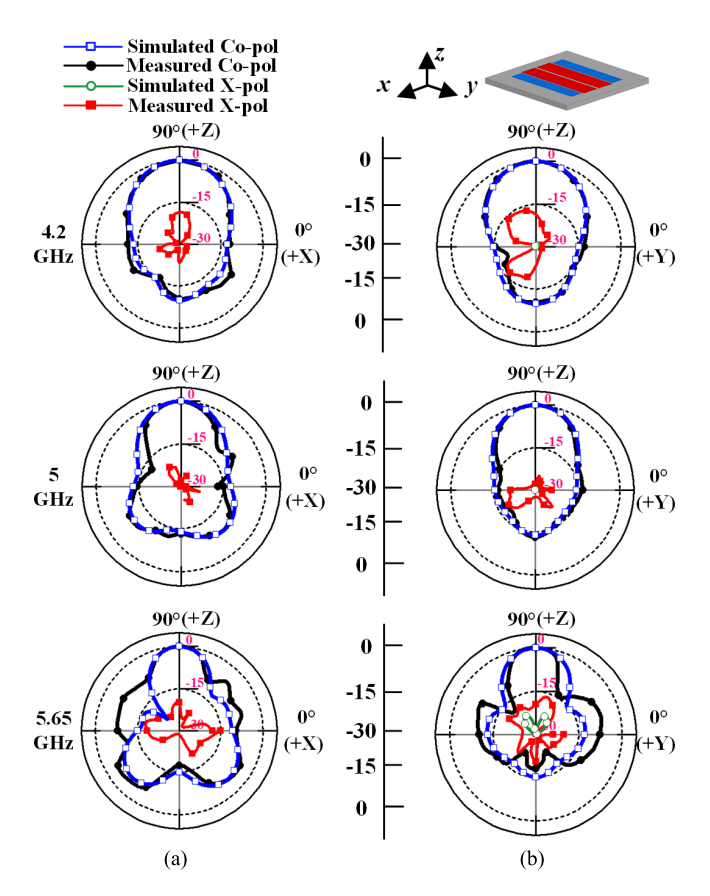


Fig. 9. Simulated and measured normalized radiation patterns of the proposed antenna at 4.2, 5, and 5.65 GHz on the (a) E-plane and (b) H-plane.

Fig. 7(a) and (b) shows its top and bottom views. A 50 Ω coaxial cable was used to feed the antenna, and the soldering positions of the inner conductor (signal line) and the outer conductor (ground) of the coaxial cable are marked in Fig. 7(b).

TABLE II

COMPARISONS OF THE PROPOSED ANTENNA WITH OTHER
PROTOTYPES IN THE LITERATURE

Ref.	Profile	Bandwidth		Peak gain
[7]	0.08 λ ₀	24%	1.40-1.78 GHz	7.2 dBi
[10]	0.145 λ ₀	31%	1.90-2.60 GHz	5 dBi
[14]	0.15 λ ₀	39%	7.60-11.30 GHz	7.8 dBi
[16]	$0.09 \lambda_0$	32.2%	4.82-6.67 GHz	6.5 dBi
[17]	$0.032 \lambda_0$	15.5%	2.32-2.70 GHz	6.8 dBi
[20]	0.07 λ ₀	31%	4.65-6.35 GHz	10 dBi
Proposed	$0.052 \lambda_0$	36.5%	3.96-5.73 GHz	10.45 dBi

 $^{^{}a}\lambda_{0}$ is the wavelength at center operating frequency in free space.

Fig. 8 reports the simulated and measured reflection coefficients, the realized gains, and the radiation efficiencies of such an antenna. The measured -10 dB impedance bandwidth is 3.96-5.73 GHz (36.5%), which is closed to the simulated result (4.01-5.82 GHz or 36.8%). The discrepancy could come from the manufacturing error or fluctuations in the substrate permittivity. The simulated peak gain is 10.7 dBi, and the simulated 3 dB gain bandwidth is 4.05-5.82 GHz (35.9%). The measured peak gain is 10.45 dBi, and the measured 3 dB gain bandwidth is 4-5.72 GHz (35.4%). Compared with the standard microstrip antenna with a peak realized gain of 7 dBi, the proposed antenna achieves a higher value of 10.45 dBi. The introduction of air gaps may enlarge the effective radiating aperture to increase the realized gain. The simulated efficiency is higher than 90%, and the measured one is higher than 79%, over the whole operating band.

Fig. 9 shows the normalized radiating patterns of the proposed antenna on the E- and H-planes at the three resonant frequencies, 4.2, 5, and 5.65 GHz. It is evidently seen that the measured copolarization is in good agreement with the simulated one. Moreover, the measured cross-polarization is less than -15 dB (-17 dB) on the E-plane (H-plane). A broadside radiation is achieved, with nearly unchanged beam direction and patterns, over the whole operating band.

Table II shows the comparison of the proposed antenna with previous works on microstrip antennas. Although the bandwidth of the design in [14] is larger than the proposed design, it has a much larger size. The antenna in [17] has a lower profile of $0.032\lambda_0$. However, its bandwidth is less than 16%. Table II clearly depicts that the proposed antenna has the widest impedance bandwidth of 36.5% and a low profile of $0.052\lambda_0$, when compared to existing broadband microstrip antennas.

V. CONCLUSION

We have presented a wideband quasi-periodic microstrip antenna based on a thin and inexpensive single-layer substrate. Specifically, the quasi-periodic radiating aperture is fed by the novel slot-to-CPW transition, which could further enhance the impedance bandwidth. By perturbing dimensions of rectangular microstrips on the quasi-periodic aperture and optimizing two branches of the slot-to-CPW transition, TM₁₀ and antiphase TM₂₀ modes can be simultaneously excited and well matched such that the operational bandwidth can be enlarged. This CPW-based feeding structure also enables designing radiation and feeding elements on a single-layer substrate, showing clear advantages over conventional multilayered wideband microstrip antennas, in terms of cost, fabrication complexity, and compactness. Our measurement results show that a broad bandwidth from 3.96 to

5.73 GHz can be achieved, even though the antenna has a total thickness of only $0.052\lambda_0$. Such compact, wideband and low-cost microstrip antenna shows great potential in many broadband communication systems.

REFERENCES

- K. L. Wong, Compact and Broadband Microstrip Antennas, New York, NY, USA: Wiley, 2002.
- [2] R. Garg, P. Bhartia, I. Bahl, and A. Ittipiboon, *Microstrip Antenna Design Handbook*. Boston, MA, USA: Artech House, 2001
- [3] E. Chang, S. Long, and W. F. Richards, "An experimental investigation of electrically thick rectangular microstrip antennas," *IEEE Trans. Antennas Propag.*, vol. AP-34, no. 6, pp. 767–772, Jun. 1986.
- [4] K.-F. Lee and K.-F. Tong, "Microstrip patch antennas-basic characteristics and some recent advances," *Proc. IEEE*, vol. 100, no. 7, pp. 2169–2180, Jul. 2012.
- [5] H. W. Lai and K. M. Luk, "Design and study of wide-band patch antenna fed by meandering probe," *IEEE Trans. Antennas Propag.*, vol. 54, pp. 564–571, 2006.
- [6] Y. Chen, S. Yang, and Z. Nie, "Bandwidth enhancement method for low profile E-shaped microstrip patch antennas," *IEEE Trans. Antennas Propag.*, vol. 58, no. 7, pp. 2442–2447, Jul. 2010.
- [7] K. L. Wong and W. H. Hsu, "A broadband rectangular patch antenna with a pair of wide slits," *IEEE Trans. Antennas Propag.*, vol. 49, no. 9, pp. 1345–1347, Sep. 2001.
- [8] K. Fan, Z.-C. Hao, and Q. Yuan, "A low-profile wideband substrate integrated waveguide cavity-backed E-shaped patch antenna for the QLINKPAN applications," *IEEE Trans. Antennas Propag.*, vol. 65, no. 11, pp. 5667–5676, Nov. 2017.
- [9] C. Y. D. Sim, C. C. Chang, and J. S. Row, "Dual-feed dual-polarized patch antenna with low cross polarization and high isolation," *IEEE Trans. Antennas Propag.*, vol. 57, no. 10, pp. 3405–3409, Oct. 2009.
- [10] M. Khan and D. Chatterjee, "Characteristic mode analysis of a class of empirical design techniques for probe-fed U-slot microstrip patch antennas," *IEEE Trans. Antennas Propag.*, vol. 64, no. 7, pp. 2758–2770, Jul. 2016.
- [11] A. U. Zaman, L. Manholm, and A. Derneryd, "Dual polarised microstrip patch antenna with high port isolation," *Electron. Lett.*, vol. 43, no. 10, pp. 551–552, May 2007.
- [12] F. Croq and A. Papiernik, "Large bandwidth aperture coupled microstrip antenna," *Electron. Lett.*, vol. 26, no. 16, pp. 1293–1294, 1990
- [13] S. Mestdagh, W. D. Raedt, and G. A. E. Vandenbosch, "CPW-fed stacked microstrip antennas," *IEEE Trans. Antennas Propag.*, vol. 52, no. 1, pp. 74–83, Jan. 2004.

- [14] S. K. Pavuluri, C. Wang, and A. J. Sangster, "High efficiency wide-band aperture-coupled stacked patch antennas assembled using millimeter thick micromachined polymer structures," *IEEE Trans. Antennas Propag.*, vol. 58, no. 11, pp. 3616–3621, Nov. 2010.
- [15] S. Xiao, B.-Z. Wang, W. Shao, and Y. Zhang, "Bandwidth-enhancing ultralow-profile compact patch antenna," *IEEE Trans. Antennas Propag.*, vol. 53, no. 11, pp. 3443–3447, Nov. 2005.
 [16] H. Wong, K. K. So, and X. Gao, "Bandwidth enhancement of
- [16] H. Wong, K. K. So, and X. Gao, "Bandwidth enhancement of a monopolar patch antenna with V-shaped slot for car-to-car and WLAN communications," *IEEE Trans. Veh. Technol.*, vol. 65, no. 3, pp. 1130–1136, Mar. 2016.
- [17] N.-W. Liu, L. Zhu, W.-W. Choi, and J.-D. Zhang, "A low-profile aperture-coupled microstrip antenna with enhanced bandwidth under dual resonance," *IEEE Trans. Antennas Propag.*, vol. 65, no. 3, pp. 1055– 1062, Mar. 2017.
- [18] N.-W. Liu, L. Zhu, and W.-W. Choi, "A differential-fed microstrip patch antenna with bandwidth enhancement under operation of TM 10 and TM 30 modes," *IEEE Trans. Antennas Propag.*, vol. 65, no. 4, pp. 1607–1614, Apr. 2017.
- [19] Y. M. Pan, P. F. Hu, X. Y. Zhang, and S. Y. Zheng, "A low-profile high-gain and wideband filtering antenna with metasurface," *IEEE Trans. Antennas Propag.*, vol. 64, no. 5, pp. 2010–2016, May 2016.
- [20] F. H. Lin and Z. N. Chen, "Low-profile wideband metasurface antennas using characteristic mode analysis," *IEEE Trans. Antennas Propag.*, vol. 65, no. 4, pp. 1706–1713, Apr. 2017.
- [21] W. Liu, Z. N. Chen, and X. M. Qing, "Metamaterial-based low-profile broadband aperture coupled grid-slotted patch antenna," *IEEE Trans. Antennas Propag.*, vol. 63, no. 7, pp. 3325–3329, Jul. 2015.
- [22] Q. Zheng, C. Guo, and J. Ding, "Wideband low-profile aperture-coupled circularly polarized antenna based on metasurface," *Int. J. Microw.* Wireless technol., vol. 10, no. 7, pp. 851–859, 2018.
- [23] Y. Li, W. Y. Sun, and Y. J. He, "Low-profile and dual-polarized microstrip antennas," in *Proc. 2nd URSI Atlantic Radio Sci. Conf. (URSI AT-RASC)*, Gran Canaria, Spain, 2018, pp. 1–4.
- [24] N. Bishop, W. Baron, J. Miller, J. Tuss, D. Zeppettella, and M. Ali, "Aperture coupled MEMS reconfigurable pixel patch antenna for conformal load bearing antenna structures (CLAS)," in *Proc. IEEE Antennas Propag. Soc. Int. Symp.*, Memphis, TN, USA, Jul. 2014, pp. 1091–1092.
- [25] M. D. Wright, W. Baron, J. Miller, J. Tuss, D. Zeppettella, and M. Ali, "MEMS reconfigurable broadband patch antenna for conformal applications," *IEEE Trans. Antennas Propag.*, vol. 66, no. 6, pp. 2770–2778, Jun. 2018.
- [26] Y. Li, Z. Zhang, W. Chen, Z. Feng, and M. F. Iskander, "A dual-polarization slot antenna using a compact CPW feeding structure," *IEEE Antennas Wireless Propag. Lett.*, vol. 9, pp. 191–194, 2010.
- [27] Y. Li, Z. Zhang, W. Chen, and Z. Feng, "Polarization reconfigurable slot antenna with a novel compact CPW-to-slotline transition for WLAN application," *IEEE Antennas Wireless Propag. Lett.*, vol. 9, pp. 252–255, 2010.